British Journal of Mathematics & Computer Science
4(23): 3312-3327, 2014
ISSN: 2231-0851

SCIENCEDOMAIN *international*
www.sciencedomain.org

A Computational Study on the Viscous in Compressible Laminar Separated Flow in a Unit Square Cavity

Pulakesh Sen[1*] and Sanjib Kumar Datta[2*]

[1]Department of Mathematics, D.N.C. College, P.O.- Aurangabad, Dist.- Murshidabad, PIN-742201, West Bengal, India.
[2]Department of Mathematics, University of Kalyani, P.O.-Kalyani, Dist.- Nadia, PIN- 741235, West Bengal, India.

Article Information

DOI: 10.9734/BJMCS/2014/12573
Editor(s):
(1) Sheng Zhang, Department of Mathematics, Bohai University, Jinzhou, China.
Reviewers:
(1) Anonymous
(2) Anonymous
Peer review History: http://www.sciencedomain.org/review-history.php?iid=669&id=6&aid=6202

Original Research Article

Received: 07 July 2014
Accepted: 18 August 2014
Published: 24 September 2014

Abstract

The phenomenon of Fluid flow separation is associated with a number of Fluid Flow Problems faced in real life situation nowadays. To understand these flow problems even under the assumption of the incompressible viscous flow is quiet a difficult task. The complexity lies on the wide variety of laminar separated flows depending on the body shape, several low and high Reynolds number, surface roughness, transition, etc. Several attempts have been made to solve the complete unsteady Navier–Stokes equations for low Re-Laminar flow problems using a variety of formulations. Among them the vorticity-stream function and pressure–velocity formulations are widely used. In this work a type of steady–state incompressible laminar flow problem in a lid-driven unit square cavity has been studied which deals with different low and high Re. For solving this problem attempts have been made to predict the flow characteristics in a uniform laminar cavity of unit square area by solving the full time dependent, Two–dimensional Navier–Stokes equations in Primitive variable formulations. The methods applied in this study can be carried out in different types of Laminar and Turbulent flows raised in our real life situations.

Keywords: Laminar flow, Reynolds number (Re), navier-stokes' equation, pressure poisson equation, streamline, iso-vorticityline, stability criteria.

MSC-Subject classification: 76 A 02, 76 D 03.

**Corresponding author: psendnc2011@gmail.com, sanjib_kr_datta@yahoo.com;*

1 Introduction

The wide variety of fluid flow problems are divided broadly into two types of flow depending on the Reynolds number which are Laminar flows associated with low Reynolds numbers and Turbulent flows associated with high Reynolds numbers. And this whole range of fluid flows can be represented by the complete Navier-Stokes equations provided the flow is sufficiently continuous and differentiable in a certain domain of space and time. But, unfortunately it is not yet possible to solve the complete Navier-Stokes equations for fluid flow problems under all kind of initial and boundary conditions. However, already a broad level of successes has been achieved for laminar flow problems. To get a description of laminar separated flow problems, earlier solvers have used pressure Poisson equations or pressure correction terms for determining pressure. But to improve the efficiency of the iteration process, a two-stage algorithm has been developed which is used in this study. In this study, computations have been performed with the help of the Bi-CG-Stab (Bi-Conjugate Gradient Stabilized) method due to the algorithm given in [1]. Here the velocity components are zero on the left, right and bottom walls of the cavity but on the upper wall the u-velocity is changing as the upper lid is moving with a speed-*u*, defined by

$$u(x) = -16x^2(1-x)^2, x \in [0,1] \tag{1.1}$$

The flow patterns, flow separations (using the upper and lower wall vorticity lines) are observed in the Figures for different Re. Through the Tables the comparison of numerical results using different schemes mentioned in [2] with the present scheme is shown as well as the effects of Reynolds numbers on the average vorticity, stream-functions, u-velocity at the centerline, points of flow separation on the lower and upper walls are studied here.

2 Governing Equations

In the investigated 2-D laminar flow problem, the fundamental equations that govern the unsteady incompressible flow of a Newtonian fluid with some constant properties in their conservative form due to [3] which are found as well in [4,5] having no body forces, are as follows:

The continuity equation:

$$\frac{\partial u}{\partial x} + \frac{\partial v}{\partial y} = 0 \tag{2.1}$$

The u – momentum equation:

$$\frac{\partial u}{\partial t} + \frac{\partial u^2}{\partial x} + \frac{\partial uv}{\partial y} = -\frac{1}{\rho}\frac{\partial p}{\partial x} + \frac{\mu}{\rho}\left(\frac{\partial^2 u}{\partial x^2} + \frac{\partial^2 u}{\partial y^2}\right) \tag{2.2}$$

And the v – momentum equation:

$$\frac{\partial v}{\partial t} + \frac{\partial uv}{\partial x} + \frac{\partial v^2}{\partial y} = -\frac{1}{\rho}\frac{\partial p}{\partial y} + \frac{\mu}{\rho}\left(\frac{\partial^2 v}{\partial x^2} + \frac{\partial^2 v}{\partial y^2}\right) \tag{2.3}$$

where (u,v) = velocity components along (x,y) – directions, p = pressure, ρ = density of the fluid and μ = coefficient of viscosity.

The non – dimensional form of the above equations are as follows:
The continuity equation:

$$\frac{\partial u}{\partial x}+\frac{\partial v}{\partial y}=0 \tag{2.4}$$

The u – momentum equation:

$$\frac{\partial u}{\partial t}+\frac{\partial u^2}{\partial x}+\frac{\partial uv}{\partial y}=-\frac{\partial p}{\partial x}+\frac{1}{\mathrm{Re}}\left(\frac{\partial^2 u}{\partial x^2}+\frac{\partial^2 u}{\partial y^2}\right) \tag{2.5}$$

And the v – momentum equation:

$$\frac{\partial v}{\partial t}+\frac{\partial uv}{\partial x}+\frac{\partial v^2}{\partial y}=-\frac{\partial p}{\partial y}+\frac{1}{\mathrm{Re}}\left(\frac{\partial^2 v}{\partial x^2}+\frac{\partial^2 v}{\partial y^2}\right), \quad \mathrm{Re}=\frac{U.L.\rho}{\mu}. \tag{2.6}$$

3 Initial and Boundary Conditions

There is no flow initially inside the flow domain (unit square cavity) while there is some specified form of velocity at the upper wall boundary of the cavity. This physically represents that the flow is initiated by the motion of the upper boundary wall of the unit square cavity. Because of the elliptic nature of the equations the boundary conditions surrounding the prescribed domain should be specified. Here the velocity components (u,v) are specified over the boundary of the computational domain. The pressure field is obtained from the velocity components at the boundaries. Here in this problem the velocity components (u,v) are zero on the left, right and bottom walls of the cavity and the u-velocity is given by the Equation (1.1) on the upper wall boundary.

4 Type of Grid and Grid Independence

A typical grid alignment is taken in the computational domain of the cavity where it is discretized via structured, uniform grid distributions with specified boundary conditions. The staggered grids are employed to this method which is known as MAC-Cell (Marker and Cell Method) due to [3]. In this grid alignment the velocity components and pressure are evaluated at the cell positions, u–velocities at the middle of the vertical sides, v–velocities at the middle of the horizontal sides and the pressure at the center of the MAC–cell due to [6]. Several grid distributions with different mesh-size are tested to assure that the computational results are grid-independent up to 98% of accuracy. The results are shown in Table-2 in terms of u-velocity for different points of x. These phenomena of acute grid independence are very much shown in [7].

5 Mathematical Formulation

The convective and the diffusive terms are discretized using second order accurate 3–point central difference formulation in both the cases. The time derivative terms are discretized according to the first order accurate 2–level forward time difference formulations.

The difference equations representing the continuity equation in the uniform grid - spacing for a typical cell (i,j) is given by

$$\frac{u_{ij} - u_{i-1\,j}}{\delta x} + \frac{v_{ij} - v_{ij-1}}{\delta y} = 0 \tag{5.1}$$

The finite difference equations approximating the momentum equations in the finite difference method (FDM) for the uniform grid – spacing are

$$\frac{u^{n+1}{}_{ij} - u^{n}{}_{ij}}{\delta t} = -\frac{p^{n}{}_{i+1\,j} - p^{n}{}_{ij}}{\delta x} + uot^{n}{}_{ij} \tag{5.2}$$

$$uot^{n}{}_{ij} = \frac{1}{\mathrm{Re}}\left[\frac{u^{n}{}_{i+1\,j} - 2u^{n}{}_{ij} + u^{n}{}_{i-1\,j}}{\delta x^{2}} + \frac{u^{n}{}_{ij+1} - 2u^{n}{}_{ij} + u^{n}{}_{ij-1}}{\delta y^{2}}\right]$$

Where $-(1-\alpha)\dfrac{u^{n}{}_{r}u^{n}{}_{r} - u^{n}{}_{l}u^{n}{}_{l}}{\delta x} - \alpha\dfrac{u^{n}{}_{r}\phi^{n}{}_{ur} - u^{n}{}_{l}\phi^{n}{}_{ul}}{\delta x}$ in the x – direction.

$$-(1-\alpha)\frac{v^{n}{}_{t}u^{n}{}_{t} - v^{n}{}_{b}u^{n}{}_{b}}{\delta y} - \alpha\frac{v^{n}{}_{t}\phi^{n}{}_{ut} - v^{n}{}_{b}\phi^{n}{}_{ub}}{\delta y}$$

And

$$\frac{v^{n+1}{}_{ij} - v^{n}{}_{ij}}{\delta t} = -\frac{p^{n}{}_{ij+1} - p^{n}{}_{ij}}{\delta y} + vot^{n}{}_{ij} \tag{5.3}$$

$$vot^{n}{}_{ij} = \frac{1}{\mathrm{Re}}\left[\frac{v^{n}{}_{i+1\,j} - 2v^{n}{}_{ij} + v^{n}{}_{i-1\,j}}{\delta x^{2}} + \frac{v^{n}{}_{ij+1} - 2v^{n}{}_{ij} + v^{n}{}_{ij-1}}{\delta y^{2}}\right]$$

Where $-(1-\alpha)\dfrac{u^{n}{}_{r}v^{n}{}_{r} - u^{n}{}_{l}v^{n}{}_{l}}{\delta x} - \alpha\dfrac{u^{n}{}_{r}\phi^{n}{}_{vr} - u^{n}{}_{l}\phi^{n}{}_{vl}}{\delta x}$ in the y – direction.

$$-(1-\alpha)\frac{v^{n}{}_{t}v^{n}{}_{t} - v^{n}{}_{b}v^{n}{}_{b}}{\delta y} - \alpha\frac{v^{n}{}_{t}\phi^{n}{}_{vt} - v^{n}{}_{b}\phi^{n}{}_{vb}}{\delta y}$$

The constant coefficient ‘α’ in the above expressions gives the desired amount of upstream or donor cell differencing i.e. when α is zero, these difference equations (5.1-5.3) are centered in space and correspond to the original MAC–formulation [3]. Those centered equations are numerically unstable and normally require some viscosity terms to be stable. When α is equal to unity the equations reduce to the full upstream or donor cell form which is conditionally stable.

The present algorithm involves the Poisson equation of pressure in order to model the elliptic nature of the pressure field in a suitable manner. This pressure Poisson equation can be derived either by differentiation and followed by the addition of the momentum equations or by combining the discretized form of the continuity and momentum equations as mentioned earlier. The final expression of the pressure Poisson equation in case of uniform grid is given here as follows:

$$\frac{p^n{}_{i+1j} - 2p^n{}_{ij} + p^n{}_{i-1j}}{\delta x^2} + \frac{p^n{}_{ij+1} - 2p^n{}_{ij} + p^n{}_{ij-1}}{\delta y^2} = \frac{D^n{}_{ij}}{\delta t} + \frac{uot^n{}_{ij} - uot^n{}_{i-1j}}{\delta x} + \frac{vot^n{}_{ij} - vot^n{}_{ij-1}}{\delta y} \quad (5.4)$$

6 Derivation of Pressure Poisson Equation

Basic algorithm for the solution of this equation is due to [6] who developed this method by applying the Successive over Relaxation (S.O.R) method. But the method which is being used here to solve the equation is a faster one, namely Bi–CG-Stab (Bi-Conjugate Gradient Stabilized) method. It is an iterative method and some initial specified values of the parameters are to be provided. This is done by providing the results of the previous time step. Thus after rearranging the pressure Poisson equation (5.4) it becomes

$$(a+b+c+d)\,p^n{}_{ij} - a.p^n{}_{i+1j} - b.p^n{}_{i-1j} - c.p^n{}_{ij+1} - d.p^n{}_{ij-1} = r.h.s$$

$$where, r.h.s = -\left[\frac{D^n{}_{ij}}{\delta t} + \frac{uot^n{}_{ij} - uot^n{}_{i-1j}}{\delta x_i} + \frac{vot^n{}_{ij} - vot^n{}_{ij-1}}{\delta y_j}\right] \quad (6.1)$$

$$D^n{}_{ij} = \frac{u^n{}_{ij} - u^n{}_{i-1j}}{\delta x_i} + \frac{v^n{}_{ij} - v^n{}_{ij-1}}{\delta y_j}$$

and

$$a = \left(\frac{2}{\delta x_i(\delta x_i + \delta x_{i+1})}\right), b = \left(\frac{2}{\delta x_i(\delta x_{i-1} + \delta x_i)}\right),$$

$$c = \left(\frac{2}{\delta y_j(\delta y_j + \delta y_{j+1})}\right), d = \left(\frac{2}{\delta y_j(\delta y_{j-1} + \delta y_j)}\right)$$

Here $D^n{}_{ij}$ is called the divergence of the velocity–field at the cell (i,j) at n^{th} time level which is minimized to zero for the convergence of the flow. In the derivation of the pressure Poisson equation(6.1) the divergence term ($D^n{}_{i,j}$) is retained and evaluated in the pressure Poisson iteration.

7 Numerical Stability Criteria

To reduce the calculation time the number of iterations in the above said scheme has been kept limited to a minimum number and the stability criteria (steady-state) has been induced, i.e. the

terms $\frac{\partial u}{\partial t} and \frac{\partial v}{\partial t}$ have to be minimized to zero or less than some very small number in absolute sense. To make the numerical scheme accurate, effective and numerically stable certain restrictions is followed in defining the mesh–size δx, δy and δt. Moreover for the present finite difference scheme (FDM) the combination factor α is also limited by restrictions.

After discretizing the flow domain depending on the problem on the study the time step is determined due to [7]. It is governed by two restrictions, firstly, material cannot move through more than one cell in one time step. Therefore the time – increment must satisfy the following inequality condition:

$$\delta t_1 \leq \left[\frac{\delta x}{u}, \frac{\delta y}{v} \right]_{\min} \tag{7.1}$$

Generally, δt_1 is chosen as equal to the one – fourth to that found from the above inequality condition. And the momentum must not diffuse more than one cell approximately in a single time step. From the linear stability analysis this limitation implies:

$$\delta t_2 < \frac{\mathrm{Re}}{2} \frac{\delta x^2 \delta y^2}{(\delta x^2 + \delta y^2)} \tag{7.2}$$

A factor of 0.8 is multiplied with the δt_2 which is found from the above inequality condition due to [8]. Thus finally the time step which satisfies above two inequality conditions is selected. The time step actually used in the computations is determined from the relation

$$\delta t = \mathrm{FCT}. [\ \mathrm{Min}\ (\ \delta t_1, \delta t_2\ )], \quad \mathrm{FCT} \in [0.2, 0.4] \tag{7.3}$$

As earlier mentioned for the present illustrated finite difference formulation, there is another parameter which is very much needed to ensure the stability of the scheme. This parameter is α, the combination factor of two finite difference schemes. The proper choice of this parameter α is governed by the inequality condition mentioned below:

$$1 \geq \alpha > \left[\left| \frac{u \delta t}{\delta x} \right|, \left| \frac{v \delta t}{\delta y} \right| \right]_{\max} \tag{7.4}$$

And α is taken approximately 1.2 times larger than what is found from the above inequality condition.

8 Numerical Results and Discussion

In this study several numerical results on the average vorticity, stream-functions, u-velocity at the centerline, points of flow separation on the lower and upper walls have been obtained for 2-dimensional laminar flow in the unit square cavity for different Reynolds numbers (Re=10,400,800,1200,2000) which are illustrated through several tables and figures.

Table 1 shows the comparison of flow predictions of different schemes as mentioned in [2] with the present scheme. This includes the comparison of the stream function ψ (maximum value), averaged value of the vorticity on the upper wall of the cavity ($\int_0^1 \omega(x,1)dx$) and the maximum u – velocity at x = 0.5). The results obtained in this work agree well with the available results in [2] as evidenced in Table 1 which proves the correctness of the scheme. Table 2 shows the grid-independence of the method with respect to the grid-sizes 40, 80 and 160 up to an accuracy of 98%. Table 3 illustrates the effect of Re on the averaged value of the vorticity on the upper wall of the cavity. We observe that the value of averaged vorticity increases with Re. Table 4 shows the effect of Re on the stream function ψ. The maximum value of ψ decreases slightly with the Re and the points (*x, y*) where ψ is maximum come closer to the middle of the unit square cavity. Table 5 shows the effect of Re on the CPU processing time of the computational program used and on the number of its iterations. It indicates that the higher Re increases the complicacy of the computational process by taking more time and iteration to get the steady-state and divergence criteria satisfied as in [9]. Table 6 shows the separation of the flow at different Re on the lower wall of the unit square cavity. It indicates that the flow separates at two different points on the lower boundary (y = 0) nearer to the left and the right walls respectively. The points also move towards the middle of the lower boundary. In case of the upper wall flow separation, the flow separates at two different points (for Re = 10, 100)but the flow separates only at a single point on the upper wall (for Re=400,1200,2000).

The Schematic diagram is shown in the Fig. 1 which illustrates the 2-D Geometry of the unit square cavity with specified boundary conditions. The upper wall vorticity lines for different Re are shown in the Fig. 2. The point on the upper wall boundary where the vorticity vanishes indicates the points of separations. It is observed that the flow separates at one point on the upper wall of the unit square cavity; whereas in case of lower wall vorticity lines we observe that the flow separates at two different points on the lower wall as shown in the Fig. 3. From both the figures it is evident that the points of separations move towards the middle of the upper and lower wall boundaries of the cavity and the length of flow separation decreases with the increase of Re. The Fig. 4 illustrates the behavior of the u-velocity at the centerline (x = 0.5) and it is observed that u-velocity is positive in the right hand side of the centerline which gradually becomes negative in the left hand side of the centerline. The points where u-velocity vanishes, shifts towards the bottom wall of the unit square cavity as Re increases. The behavior of the vertical v-velocity is also investigated at the centerline (y = 0.5) as shown in the Fig. 5. The patterns of the streamlines and constant vorticity lines are shown in different figures (from Figs. 6 to 13) for low and high Re. Fig. 6 shows the streamlines corresponding to ψ = 0, 0.01, 0.02, 0.03, 0.04, 0.05, 0.06, 0.07 and 0.08. Those streamlines shift towards the left - upper corner of the unit square cavity as Re increases as shown in Figs. 7, 8, 9 respectively. The constant vorticity lines at the Fig. 10 indicate that the vorticity expands towards the upper wall of the unit square cavity. Other figures consisting of iso-vorticity lines as shown in Figs. 11, 12 and 13 also agree with the first one and it can be decided that the lines moves towards the left upper corner of the cavity and the density of those iso-vorticity lines increases adjacent to the upper wall.

Table 1. Comparison of various schemes for laminar cavity flow predictions (for Re = 400, δx = δy = 0.05)

Sl. no	Scheme	$\underset{(x,y)}{Max}\Psi(x,y)^a$	$\int_0^1 \omega(x,1)dx$	$\underset{y}{Max}\,u(0.5,y)$
1.	Run – 1[b]	0.0632	7.62	0.132
2.	Run – 6[b]	0.0750	6.94	0.188
3.	Run – 7[b]	0.0718	7.55	0.173
4.	Run – 8[b]	0.0677	7.35	0.141
5.	Present scheme	0.0689	7.23	0.161

[a]Obtained for x = 0.35, y = 0.75 (Run –1); x = 0.35, y = 0.70 (Run – 8); x = 0.40,y = 0.65 (Runs – 6,7) for x = 0.40, y = 0.60 (Present scheme).[b]Peyret and Taylor (1982) , page no. 202

Table 2. Comparison of U – velocity for different grid sizes (40×40, 80×80, 160×160) at y = 0.5 for different x form 0-1.0, (Re = 400)

Grid-size	For x→	0	0.125	0.25	0.375	0.5	0.625	0.75	0.875	1.0
40X40	U =	0	0.1603	0.2308	0.1962	0.1638	0.1275	0.0784	0.0257	0
80X80	U =	0	0.1691	0.2316	0.1892	0.1601	0.1292	0.0817	0.0268	0
1160X160	U =	0	0.1742	0.2952	0.1820	0.1623	0.1209	0.0795	0.0243	0

Table 3. Effect of Reynolds numbers on averaged value of vorticity

Sl. no	Reynolds no	$\int_0^1 \omega(x,1)dx$ (Averaged vorticity)
1.	10	4.2842
2.	100	4.9875
3.	400	7.6846
4.	1200	11.6767
5.	2000	14.2606

Table 4. Effects of Reynolds numbers on the stream function: $(\Psi)_{max}$

Sl. no	Reynolds no.	Ψmax	x	y
1.	10	0.08295	0.475	0.775
2.	100	0.08217	0.4	0.75
3.	400	0.07900	0.4	0.625
4.	1200	0.07026	0.45	0.55
5.	2000	0.06360	0.45	0.55

Table 5. Effect of Reynolds numbers on the iteration no. and time (for 40×40 grid -points)

Sl. no	Reynolds no	No. of iterations	Real time (M:S)	CPU time (M:S)
1.	10	5337	1: 22.63	1: 24.71
2.	100	5032	1: 08.71	1: 10.51
3.	400	7105	1: 33.76	1: 36.50
4.	1200	11508	2: 08.47	2: 12.25
5.	2000	13749	2: 23.96	2: 28.34

Table 6. Effect of Reynolds number on the flow separation at lower and upper walls (for 40×40-grid points) flow separation at different points

Sl. no	Re	Lower wall (x)	Upper wall (x)
1.	10	0.08, 0.92	0.06, 0.95
2.	100	0.15. 0.92	0.25, 0.98
3.	400	0.21, 0.89	0.31, [a]X
4.	1200	0.26, 0.79	0.27, [a]X
5.	2000	0.26, 0.75	0.25, [a]X

[a]X – No separation on the upper wall (near the right wall boundary).

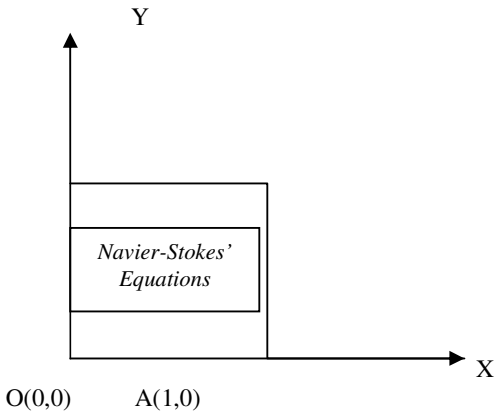

Fig. 1. A schematic diagram of the unit square cavity

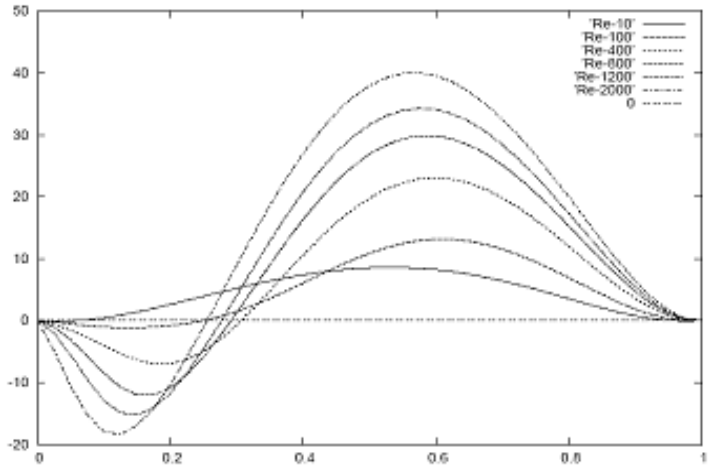

Fig. 2. Distribution of upper wall vorticity for Re= 10,100,400,800,1200,2000

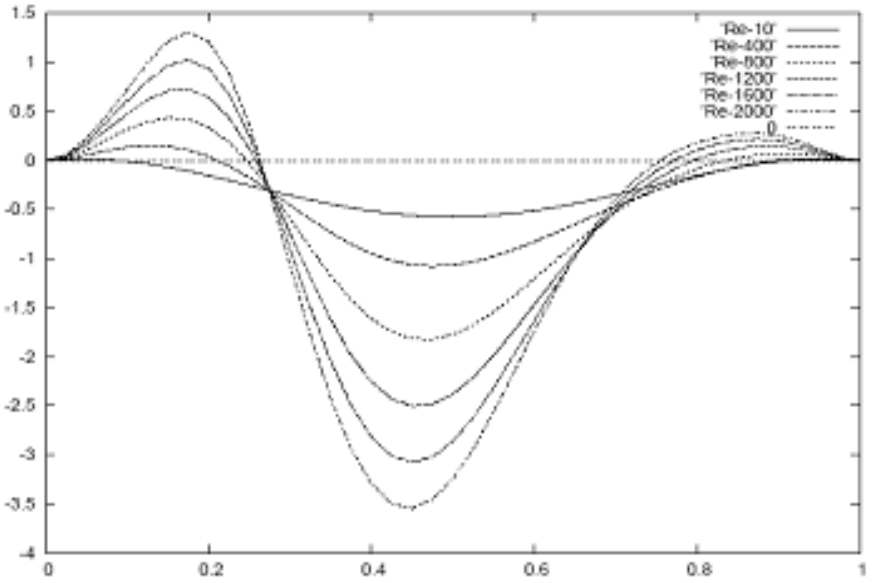

Fig. 3. Distribution of lower wall vorticity for Re= 10, 100, 400, 800, 1200, 2000

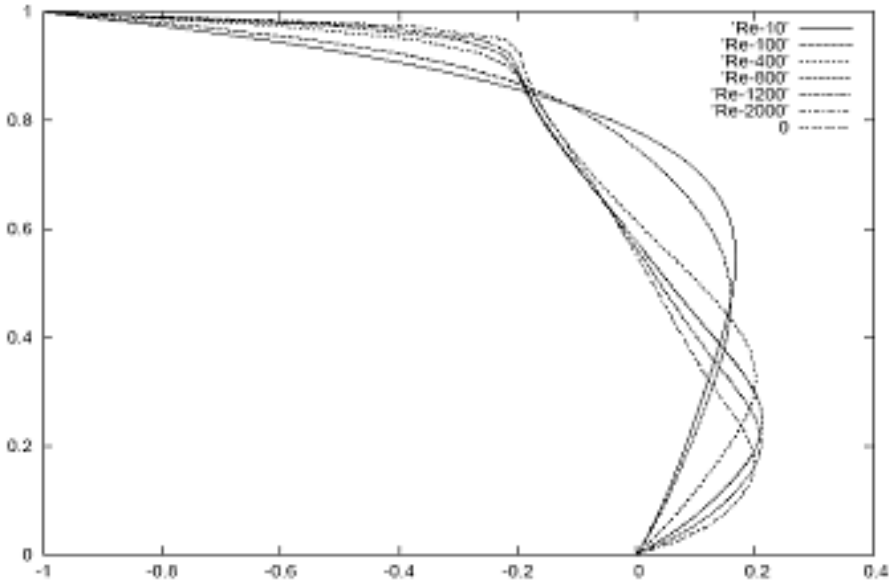

Fig. 4. The u-velocity on the line x=0.5 for Re= 10, 100, 400, 800, 1200, 2000

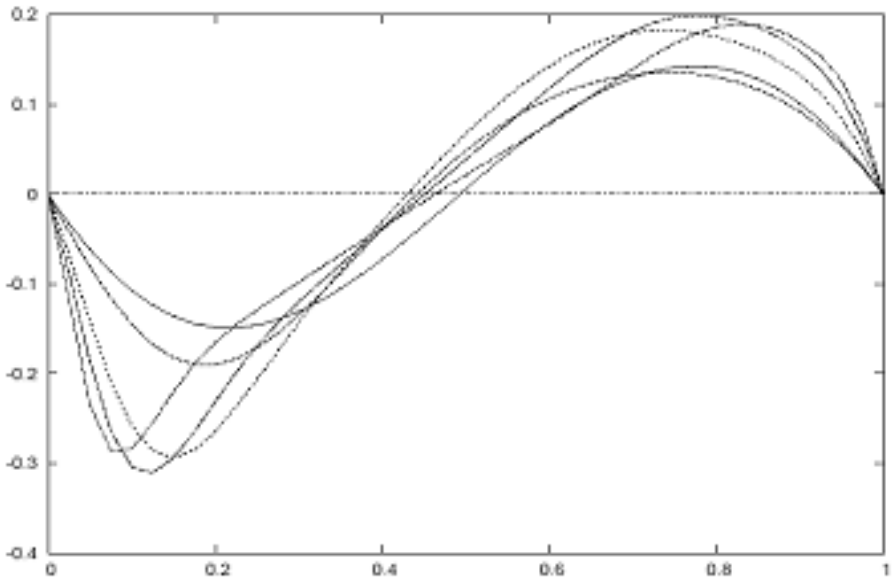

Fig. 5. The u-velocity on the line x=0.5 for Re= 10, 100, 400, 800, 1200, 2000

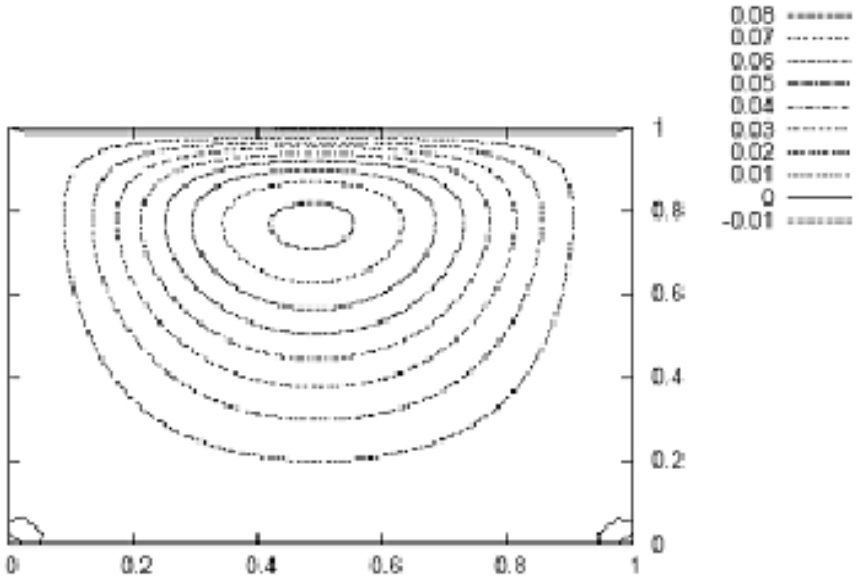

Fig. 6. Streamlines for laminar flow in the cavity, Re = 10

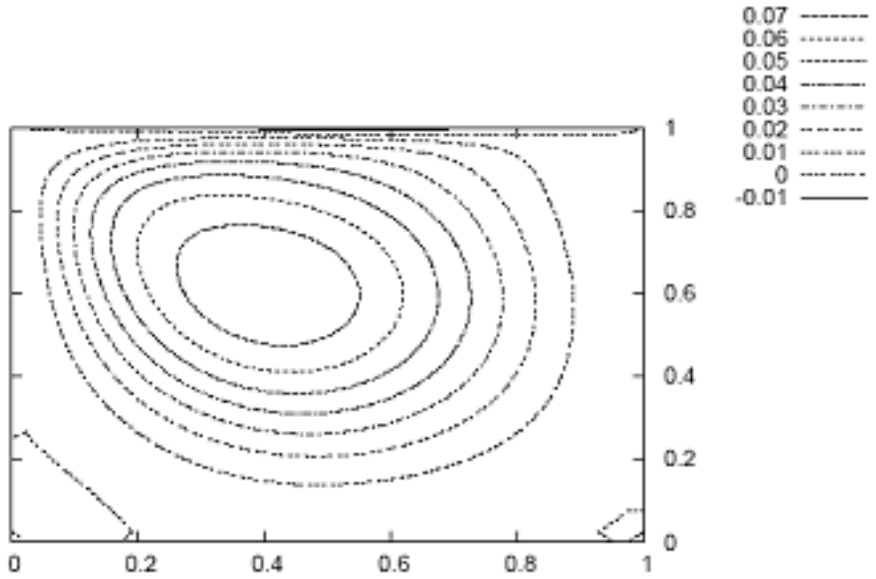

Fig. 7. Streamlines for laminar flow in the cavity, Re = 400

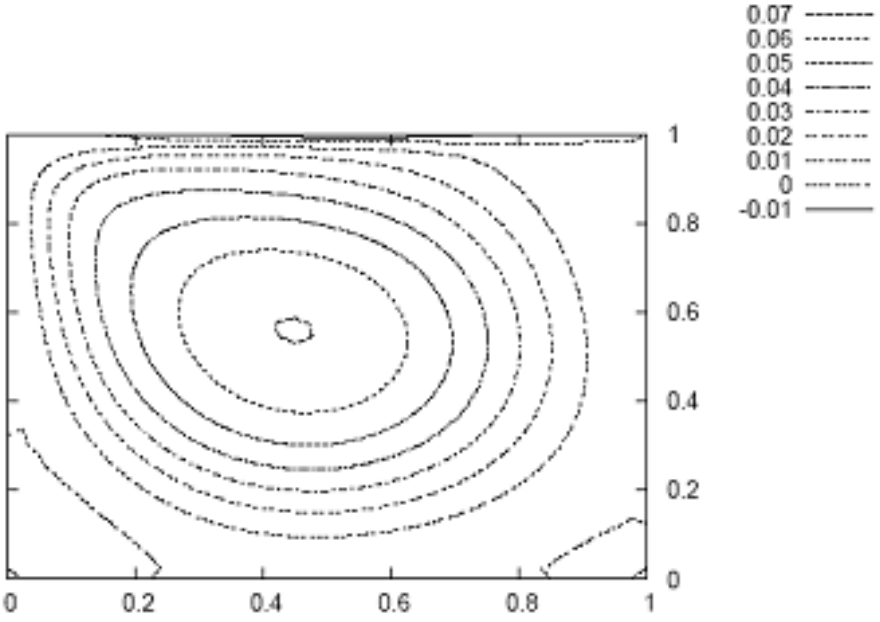

Fig. 8. Streamlines for laminar flow in the cavity, Re = 1200

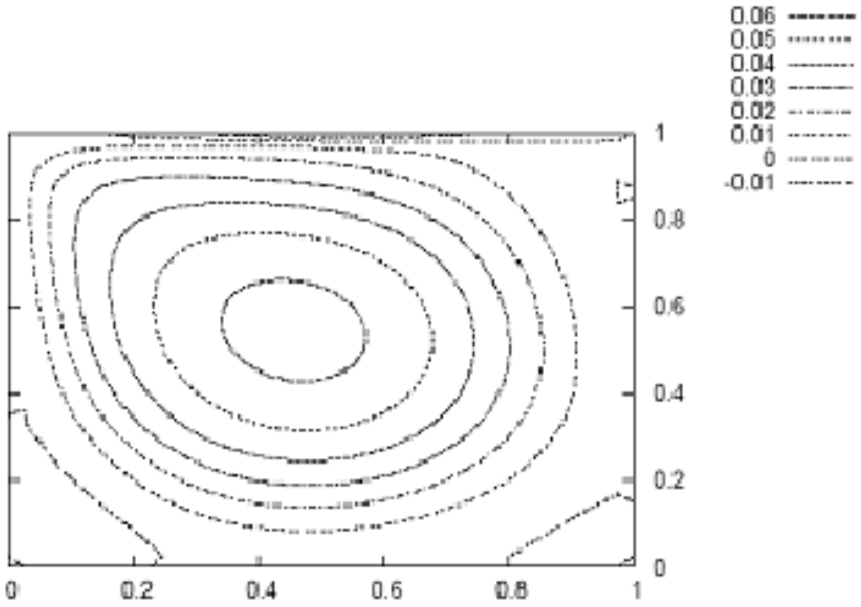

Fig. 9. Streamlines for laminar flow in the cavity, Re = 2000

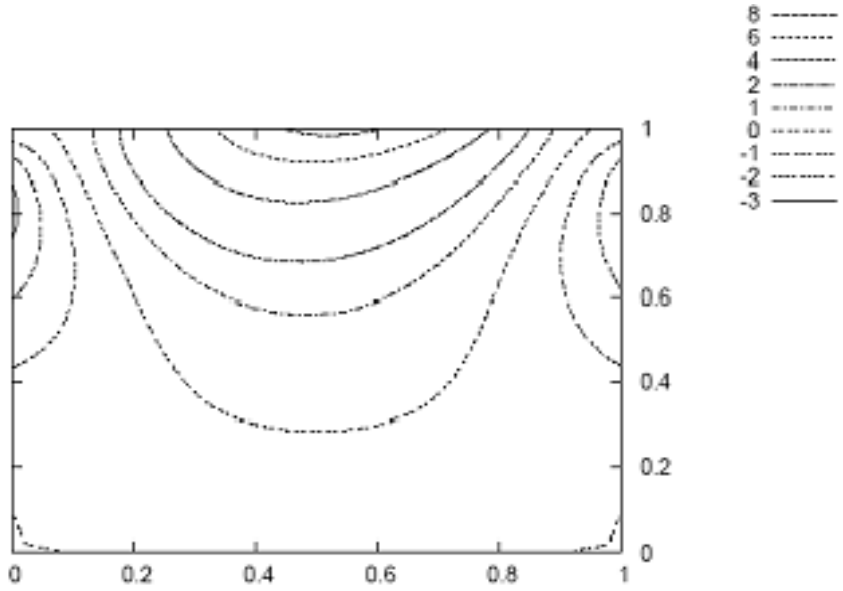

Fig. 10. Constant-vorticity lines in the cavity, Re= 10

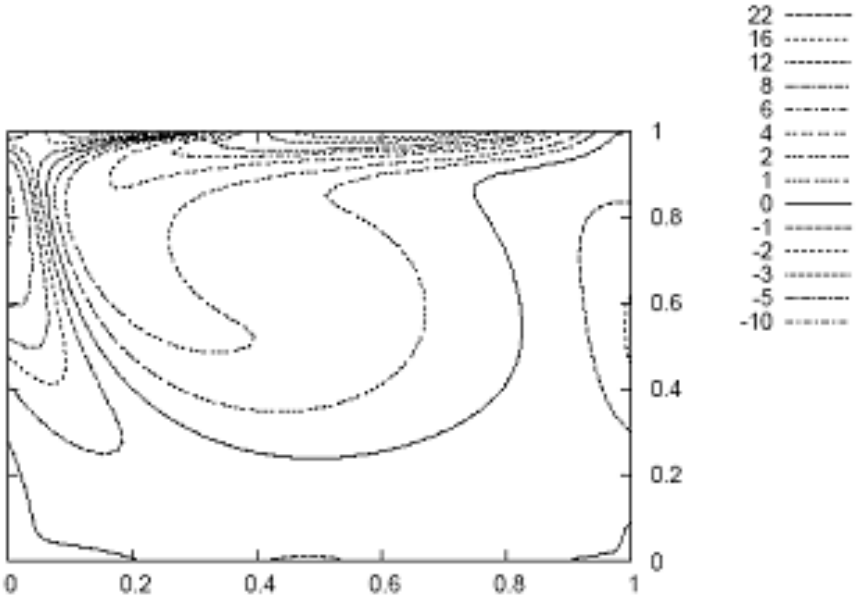

Fig. 11. Constant-vorticity lines in the cavity, Re= 400

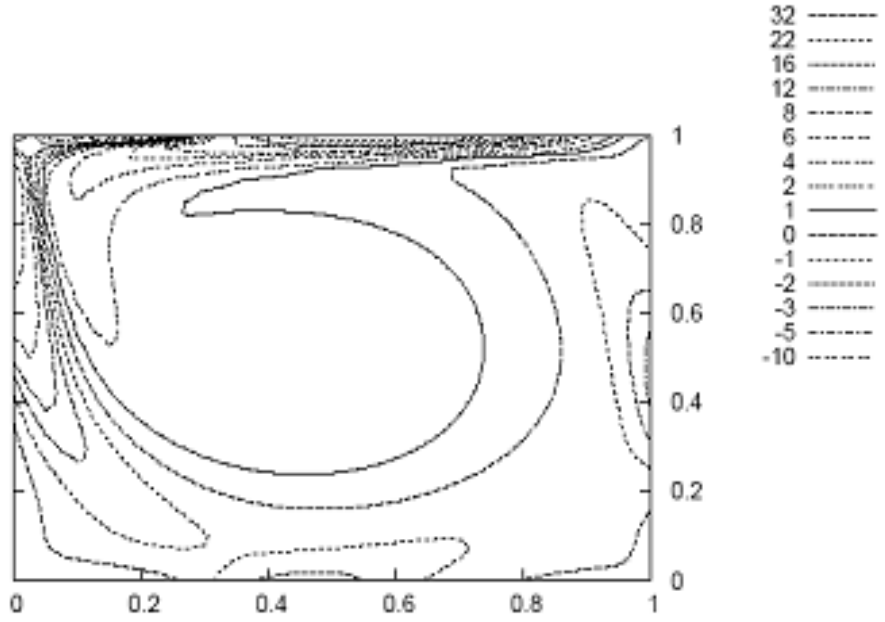

Fig. 12. Constant-vorticity lines in the cavity, Re= 1200

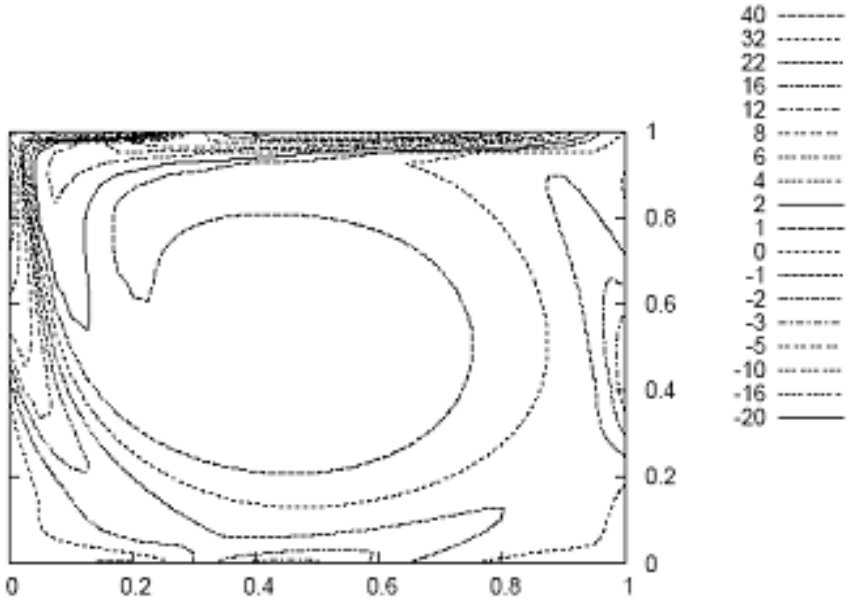

Fig. 13. Constant-vorticity lines in the cavity, Re= 2000

9 Conclusion

The present study investigated a laminar separated flow in a unit square cavity with specified boundary conditions over the domain. The Finite Difference method using staggered grid is applied to discretize the continuity and momentum equations. The grid-independence of the method is also shown here. The pressure Poisson equation is solved till convergence using Bi-CG-Stab method, a numerical method which solves a system of equations quite faster than any other methods. Our results agree well with available results mentioned at different research work. The flow characteristics are identified and presented here with the above tables and figures. The behavior of velocity components, streamlines, iso-vorticity lines, upper and lower wall vorticity distributions in the unit square cavity are investigated throughout this study. It is observed that the patterns of streamlines change from low to high Reynolds no. and the flow separation points shifts towards the mid-point of the lower and upper wall with the increase of Re. The iso-vorticity lines become dense near the upper wall as Re increases. The u and v-velocities are also figured out for different Re. The computational results are obtained and produced through several tables and figures at the last section of the above characterizing the whole effort. The methods applied in this study and the results obtained can be carried out in different types of Laminar and Turbulent flows raised in our real life situations henceforth.

Acknowledgments

The work of the present paper is an output of the M. Phil –Thesis of the first author under the supervision of Dr. T. R. Mahapatra, Associate Professor, Department of Mathematics, Visva-

Bharati, Santiniketan, India. The first author gratefully acknowledges the enormous help and guidance of Dr. Mahapatra to work on this topic and is indebted to him for his kind support and valuable suggestions in this regard.

Competing Interests

Authors have declared that no competing interests exist.

References

[1] Kelley CT. Iterative methods for linear and non–linear equations. Society for Industrial and Applied Mathematics, Philadelphia. 1995;1-3:3-62.

[2] Peyret R, Taylor TD. Computational methods for fluid flow. Springer-Verlag, New York; 1982.

[3] Harlow FH, Welch JE. Numerical solution of time dependent viscous incompressible flow of fluid with free surface. Phys Fluids. 1965;8:2182-2189.

[4] Safaei MR, Goshayeshi HR, Razavi BS, Goodarzi M. Numerical investigation of laminar and turbulent mixed convection in a shallow water-filled enclosure by various turbulence methods. Scientific Research and Essays. 2011;6(22):4826-4838.

[5] Goodarzi M, Safaei MR, Hakan FO, Karimipour A, Sadeghinezhad E, Dahari M, Kazi SN, Jomhari N. Numerical study of entropy generation due to coupled laminar and turbulent mixed convection and thermal radiation in an enclosure filled with a semi-transparent medium. The Scientific World Journal. 2014;8.

[6] Welch JE, Harlow FH, Shannon JP, Daly BJ. The MAC method. Los Alamos Scientific Laboratory Report LA-3425; 1966.

[7] Young D. Iterative methods for solving partial differential equations of elliptic type. Trans Amer Math Soc. 1954;76: 92-111.

[8] Hirt CW. Heuristic stability theory for finite difference equations. J Comp Phys. 1968;2:339-355.

[9] Mahapatra TR, Layek GC, Maiti MK. Unsteady laminar separated flow through constricted channel. International Journal of Non-Linear Mechanics. 2002;37:171-186. Pergamon.

Peer-review history:
The peer review history for this paper can be accessed here (Please copy paste the total link in your browser address bar)
www.sciencedomain.org/review-history.php?iid=669&id=6&aid=6202